Asymmetry and intermittency in the rheo-inertial transition to turbulence in pipe flow

Antoine Charles, Jorge Peixinho, Thierry Ribeiro, Sam Azimi, Vincent Rocher, Jean-Christophe Baudez, S. Amir Bahrani

▶ **To cite this version:**

Antoine Charles, Jorge Peixinho, Thierry Ribeiro, Sam Azimi, Vincent Rocher, et al.. Asymmetry and intermittency in the rheo-inertial transition to turbulence in pipe flow. Physics of Fluids, 2024, 36 (5), ⟨10.1063/5.0211807⟩. ⟨hal-04760368⟩

HAL Id: hal-04760368

https://hal.science/hal-04760368v1

Submitted on 30 Oct 2024

HAL is a multi-disciplinary open access archive for the deposit and dissemination of scientific research documents, whether they are published or not. The documents may come from teaching and research institutions in France or abroad, or from public or private research centers.

L'archive ouverte pluridisciplinaire **HAL**, est destinée au dépôt et à la diffusion de documents scientifiques de niveau recherche, publiés ou non, émanant des établissements d'enseignement et de recherche français ou étrangers, des laboratoires publics ou privés.

HAL Authorization

ACCEPTED MANUSCRIPT
Physics of Fluids
AIP Publishing
This is the author's peer reviewed, accepted manuscript. However, the online version of record will be different from this version once it has been copyedited and typeset.
PLEASE CITE THIS ARTICLE AS DOI: 10.1063/5.0211807

AIP/123-QED

Asymmetry and intermittency in the rheo-inertial transition to turbulence in pipe flow

Antoine Charles,[1] Jorge Peixinho,[2] Thierry Ribeiro,[3] Sam Azimi,[4] Vincent Rocher,[4] Jean-Christophe Baudez,[1] and S. Amir Bahrani[1, a)]

[1)] *IMT Nord Europe, Institut Mines-Télécom, Center for Energy and Environment, 59000 Lille, France*

[2)] *Laboratoire PIMM, Arts et Métiers Institute of Technology, CNRS, Cnam, PIMM, HESAM Université, 75013 Paris, France*

[3)] *Institut Polytechnique UniLaSalle, Université d'Artois, ULR 7519, 19 rue Pierre Waguet, 60000 Beauvais, France*

[4)] *SIAAP - Service public pour l'assainissement francilien, Direction Innovation, 82 avenue Kléber, 92700 Colombes, France*

ACCEPTED MANUSCRIPT
Physics of Fluids
AIP Publishing
This is the author's peer reviewed, accepted manuscript. However, the online version of record will be different from this version once it has been copyedited and typeset.
PLEASE CITE THIS ARTICLE AS DOI: 10.1063/5.0211807

Transition to turbulence in pipe has been extensively studied but is still not completely understood and even more for non-Newtonian fluids. We focus here on yield stress shear-thinning fluids and the mechanism leading to the transition in pipe, so called rheo-inertial transition to turbulence. An experimental setup has enabled us to identify flow regimes in a cylindrical pipe, using both flow visualisations and pressure drops measurements for a range of Reynolds numbers. We delimited the non-Newtonian specific regime in the laminar-turbulent transition triggered at a critical Reynolds number below the turbulent puffs onset. This pre-transition regime is associated with a velocity profile asymmetry in which its degree and position evolve as the Reynolds number increases. The origin for the stability of this rheo-inertial regime is discussed, as it could be due to a competition between the non-linear contributions of rheological behavior and flow inertia. Beyond this regime, we quantified the intermittence of puff transit, revealing the delay to turbulence. We spotted for the first time a different rheo-inertial transitional behavior in the intermittency evolution versus Reynolds number, displaying a smoother transition on a broader range. Finally, the critical Reynolds numbers for different yield-stresses are compared with previous works and the novelty is the linear increase of the delay to turbulent puffs with the yield stress.

[a)]Electronic mail: amir.bahrani@imt-nord-europe.fr

ACCEPTED MANUSCRIPT
Physics of Fluids
AIP Publishing
This is the author's peer reviewed, accepted manuscript. However, the online version of record will be different from this version once it has been copyedited and typeset.
PLEASE CITE THIS ARTICLE AS DOI: 10.1063/5.0211807

I. INTRODUCTION

The search for the limit condition of the laminar-turbulent transition with the fluid rheology is of direct industrial interest because the critical transitional velocity range is the most favourable operating range[1], as it is the best compromise between pressure drop generation and homogenization by the turbulent nature of the flow. A shear thinning flow is defined by a local viscosity stratification. Moreover, a yield stress characteristic manifests a central plug zone, in which the flow is moving at a constant velocity, and reinforces the deviation from inertial transition. The rheo-inertial transition which denotes the transition resulting from the shear-thinning, possibly yield-stress fluid, rheological behavior of a fluid should be differentiated from elastic turbulence or elasto-inertial turbulence[2], encountered typically in particle-laden flows[3]. These flows exhibit different transition behaviors, scaling as a function of the particle volume fraction and of the diameter ratio of the particle to the pipe[3], due to the competition between particle-induced perturbation and viscous effects. The addition of a small amount of polymer results in a marginal delay in the onset of turbulence, but a larger results in an early transition to an elasto-inertial turbulent state[4], with a mechanism differing from Newtonian and dominated both by fluid inertia and visco-elasticity. For such fluids, the intermittence of the Newtonian inertial transition is gradually replaced by continuous particle-induced turbulence[3,5].

Considering this time the rheo-inertial transition, Pinho and Whitelaw[6] highlighted for the first time on a shear-thinning fluid, using Laser Doppler Anemometry (LDA), a delay on the transition to turbulence with a transition appearing at a higher critical Reynolds number than the one for a Newtonian fluid, due to the rheological behavior. This delay, related to the stability increase, is likely due to a reduction in the exchange of energy between the base flow and the disturbance in the critical layer as reported by Chekila[7]. Escudier and Presti[8] also observed by LDA the presence of a delay in the transition to turbulence on yield stress and shear-thinning fluids. They also observed for the first time a new phenomenon not previously reported: a degree of asymmetry is present prior to the appearance of turbulent structures. It only appeared for the non-Newtonian fluids. The asymmetry in the axial velocity profiles disappears once the conditions to a turbulent regime are achieved. The impact of the central plug region due to the yield stress behavior is not clearly established. Peixinho *et al.*[9] compared a purely shear-thinning fluid with a shear-thinning and yield stress fluid,

AIP Publishing Physics of Fluids ACCEPTED MANUSCRIPT
This is the author's peer reviewed, accepted manuscript. However, the online version of record will be different from this version once it has been copyedited and typeset.
PLEASE CITE THIS ARTICLE AS DOI: 10.1063/5.0211807

displaying once again the delay to turbulence and the asymmetry before the intermittent regime. Hence both the shear-thinning and the yield stress behaviors increase the stability of the flow in terms of relative velocity fluctuations and friction factors. Escudier *et al.*[10] compared results obtained independently in Liverpool (UK), Nancy (FR) and Melbourne (AU) with the same LDA method for three non-Newtonian fluids. All shear-thinning fluids displayed the flow asymmetry, highly suggesting that it is inherent of the shear-thinning nature. This study also confirmed that the asymmetry of the flow must be a consequence of a fluid-dynamic mechanism rather than imperfections in the flow facilities, gravity or Coriolis effects. Esmael and Nouar[11] highlighted on a yield stress fluid the evolution of the asymmetry phenomenon along the pipe axis, showing that the degree of asymmetry increases with the radial position. It suggested the existence of a coherent structure, characterized by two counter-rotating longitudinal vortices, rather than a single periodic traveling wave. Escudier *et al.*[10] and Esmael *et al.*[11] observations are confirmed by Güzel *et al.*[12]. Numerical studies made by Roland[13] and Lopez-Carranza *et al.*[14] using stability and non-linear wave analysis methods on a shear-thinning fluid found an asymmetrical solution for a $m = 1$ fundamental azimuthal wavenumber. However they did not succeed to obtain it for $m = 2$ and $m = 3$, corresponding to experimental observations by Hof *et al.*[15]. Bahrani and Nouar[16] identified experimentally on a yield stress fluid a specific pre-transition regime, delimited using the friction factor, where the flow asymmetry start before the apparition of puffs. Wen *et al.*[17] highlighted how the asymmetry degree evolves over time and the azimuthal preferential position of the asymmetry. They explained the asymmetry as a consequence of a supercritical instability of the base flow, excluding the explanation of the transition to turbulence as a subcritical transition provoked by finite-size amplitude perturbation, which is at present still generally assumed[18,19].

The novelty of this work lies in the results obtained from a method that quantify ight intensities of visualization images, combined with pressure drops. It allowed us to identify a nonlinear asymmetric state appearing before the onset of turbulent puffs, so called rheo-inertial transition to turbulence. This permitted us to quantify the turbulence intermittency for yield stress fluid and the flow asymmetry. Specifically, we obtain the evolution laws of the turbulence intermittency versus the Reynolds number. In addition, an asymmetry degree was defined, allowing the characterisation of the asymmetry evolution over flow regimes. Finally the present results are compared with previous results and a summary is proposed

ACCEPTED MANUSCRIPT
Physics of Fluids
AIP Publishing
This is the author's peer reviewed, accepted manuscript. However, the online version of record will be different from this version once it has been copyedited and typeset.
PLEASE CITE THIS ARTICLE AS DOI: 10.1063/5.0211807

where critical Reynolds numbers are presented as a function of the Carbopol concentration or the yield stresses.

The outline of the paper is as follows: Section II presents the experimental set-up, working fluids and measuring methods. Results of the laminar-turbulent transition, the flow asymmetry, the turbulence intermittency and comparisons are discussed in Sec. III. Conclusions are then outlined in Sec. IV.

II. EXPERIMENTAL SETUP, WORKING FLUIDS AND MEASURING METHODS

The experimental setup consists in a flow loop, shown in figure 1, designed to carry out combined pressure drop measurements with direct flow visualisation of the natural uncontrolled transition to turbulence in pipe. Flow is provided by a *Moineau* eccentric rotorpump (2) (PCM) from 100 l capacity tank (1). The pump flow rate can be set between 20 and 100 l/min. An electromagnetic flowmeter Proline Promag (3) (Endress+Hauser) is placed after the pump and before the entrance of the test section and its error on the flowrate is estimated at 1 %. A flexible pipe is used to reduce pulsations in the fluid flow before the entrance in the test section. A differential pressure transducer with a range spanning from $\Delta P = 0$ to 400 mbar (Druck) enables to determine the pressure losses in the test section. The test section (4) consists in a $L = 3$ m length and $D = 25$ mm inside diameter copper tube ($L/D = 120$), immediately followed by a 180 mm length and 25 mm inside diameter visualisation transparent acrylic glass pipe (5). The establishment length L_e is verified using the Froishteter and Vinogradov correlation[20] for a Herschel-Bulkley fluid in a cylindrical pipe in the laminar regime, where $L_e = [0.23(1/n)^{0.31} - 0.4(\tau_0/\tau_w)](D/2)\rho U^{2-n} D^n/K$, with τ_w the wall shear stress, U the bulk velocity and τ_0, K, n the Herschel-Bulkley parameters. The establishment length is always inferior to the test section length ($L_e \leq 2.8$ m) in laminar and asymmetry regimes. In intermittent regimes, it is checked that the flow in the most challenging conditions is at least 75% established. A high-speed camera Fastcam Mini UX 50 (6) (Photron) with an acquisition frequency of 250 Hz faces the visualisation pipe from the side and a LED white light source (7) is placed on the opposite side of the pipe. K-thermocouples (8) located inside and outside the supply tank are used to monitor the absence of temperature drift during experiments.

ACCEPTED MANUSCRIPT
Physics of Fluids
AIP Publishing
This is the author's peer reviewed, accepted manuscript. However, the online version of record will be different from this version once it has been copyedited and typeset.
PLEASE CITE THIS ARTICLE AS DOI: 10.1063/5.0211807

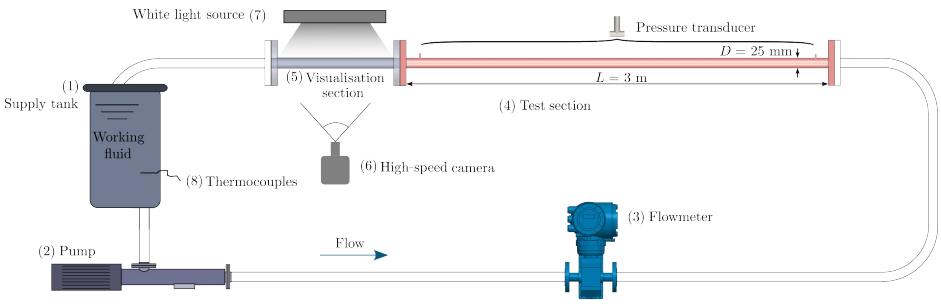

FIG. 1. Flow loop provided by a supply tank (1) and pump (2), instrumented with pressure, flowrate (3) and temperature (8) sensors, associated with a visualisation section system (5, 6, 7) immediately after the test section (4) keeping the same inner diameter to obtain simultaneously direct flow visualisation and test section pressure drop.

Different concentrations of aqueous (deionised water) neutralised Carbopol (Carb.) 940 (Acros Organics) solutions are used as working fluids. Carbopol solutions are cross-linked acrylic acid polymers forming a viscous gel, displaying well-known yield stress and shear-thinning behaviors. In the concentration range used in this work, Carbopols solutions are percolated dispersions of fully swollen micro-gels[21]. As a Newtonian reference, a 61 % glycerol/water (Gly./Wat.) mixture is used for comparison. In the present work, all the concentration are given in weight %. The rheological parameters of the working fluids are given in table I following the classical Herschel-Bulkley model ($\tau = \tau_0 + K\dot{\gamma}^n$, τ the shear stress, τ_0 the yield stress, K the consistency, $\dot{\gamma}$ the shear rate and n the flow index). Rheological characterization was performed using a thermo-regulated controlled-stress rheometer MCR 102e (Anton Paar), with a concentric cylindrical CC27 geometry and a 4.6 mm diameter gap, before and after each experiment to ensure no drift occurred. In the pipe experiments, fluids are seeded with thin and flat Iriodin 110 reflective flakes ($\sim 0.1 \times 10\,\mu$m). The light reflectance quickly responds to flow field changes, making them a great indicator of disordered flow. Moreover it has been shown by PIV comparison[22] that light intensities on visualization images from this method are linked to a radial velocity component.

A typical test is an ascending flowrate ramp. Each step is systematically maintained for seven minutes to prevent transient phenomena and the camera records the last minute. At the beginning of each ascending flowrate ramp experiment, a high flowrate is set beforehand

ACCEPTED MANUSCRIPT
Physics of Fluids
AIP Publishing
This is the author's peer reviewed, accepted manuscript. However, the online version of record will be different from this version once it has been copyedited and typeset.
PLEASE CITE THIS ARTICLE AS DOI: 10.1063/5.0211807

to avoid any residual air in the flow loop and ensure the working fluid is homogeneous. Pressure drops are measured continuously at 2 Hz. The pressure drops for each flowrate value are obtained by averaging the pressure drops over the duration of the flowrate step. The pressure drops error is estimated at 1.5 %. The visualisation images acquired are post-processed by removing the laminar background (lowest Reynolds number flow reference image) from the reference images obtained at the minimum flowrate in order to be able to distinguish variations from the base flow, while removing any undesirable optical effects.

The parietal Reynolds number (based on the diameter) $\mathcal{R}_w$ and the Fanning friction factor C_f used in the analysis are defined according to the eq. 1 and eq. 2 respectively, with ρ the fluid density, U the bulk velocity, τ_w the parietal stress and τ_0, K, n the Herschel-Bulkley fit parameters.

$$\mathcal{R}_w = \frac{4\rho U\left((\tau_w - \tau_0)/K\right)^{\frac{1}{n}}}{\Delta P/L} \quad \text{with} \quad \tau_w = \frac{D}{4}\frac{\Delta P}{L} \tag{1}$$

$$C_f = \frac{2\tau_w}{\rho U^2} \tag{2}$$

TABLE I. Rheological characterization of the working fluids.

Fluid	Model	$\mu\,(mPa\,s)$	$\tau_0\,(Pa)$	$K\,(Pa\,s^n)$	$n\,(-)$
Carb. 0.08 %	Herschel-Bulkley	-	0.06	0.23	0.61
Carb. 0.10 %	Herschel-Bulkley	-	0.48	0.38	0.58
Carb. 0.12 %	Herschel-Bulkley	-	1.49	0.82	0.53
Gly./Wat. 61/39%	Newtonian	0.018	-	-	-

III. RESULTS AND DISCUSSION

A. Laminar-turbulent transition: friction factor and flow structure

The laminar-turbulent transition flow regimes are identified using the friction factor C_f evolution versus $\mathcal{R}_w$, see figure 2, for the working fluids. A classical three stages laminar-turbulent transition is observed for the Newtonian fluid (see fig. 2 diamonds). Considering the Newtonian fluid, the laminar regime with an uniform laminar base flow without

ACCEPTED MANUSCRIPT
Physics of Fluids
AIP Publishing
This is the author's peer reviewed, accepted manuscript. However, the online version of record will be different from this version once it has been copyedited and typeset.
PLEASE CITE THIS ARTICLE AS DOI: 10.1063/5.0211807

any structures is observed for $\mathcal{R}_w < 2200$, in good agreement with the theoretical $16/\mathcal{R}_w$ Poiseuille law. The transit of turbulent puffs is then observed in the Newtonian intermittent regime, with increasing turbulence intermittence as $\mathcal{R}_w$ increase. The fully turbulent regime is reached at $\mathcal{R}_w = 2685$, with no further relaminarisation, following the Colebrook-White law with negligible roughness.

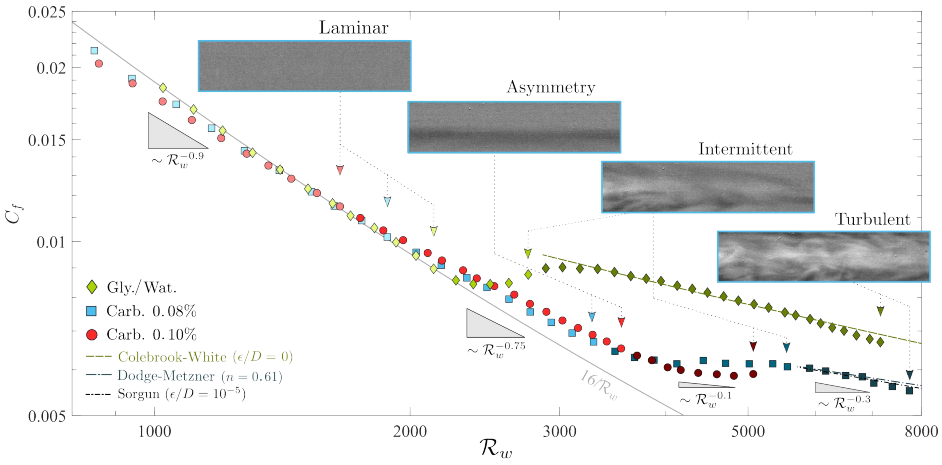

FIG. 2. Identification of flow regimes based on the friction factor C_f with the Reynolds number $\mathcal{R}_w$ for the Carb. 0.08 % (blue squares), Carb. 0.10 % (red circles) and Gly./Wat. (green diamonds). For each regime (laminar, asymmetry, intermittent and turbulent), top inserts display Carb. 0.08 % typical visualisation and the C_f dependence on $\mathcal{R}_w$ is given at the bottom. Arrows indicate the end limit of the regimes. Poiseuille, Colebrook-White, Dodge-Metzner and Sorgun *et al.*[23] reference laws are shown to demonstrate agreements with the experimental data.

Nevertheless the rheo-inertial transition to turbulence does not follow the same scenario. In this context, we observed a rheo-inertial regime in the laminar-turbulent transition for two non-Newtonian fluids (see figure 2 squares and circles). A laminar regime is observed just as for the Newtonian fluid, which follows a $C_f \sim \mathcal{R}_w^{-0.9}$ evolution. A non-Newtonian fluids specific regime is identified beyond a critical number, noted here as $\mathcal{R}_{w,c_a}$, with here $\mathcal{R}_{w,c_a} = 1955$ and $\mathcal{R}_{w,c_a} = 1700$ for Carb. 0.08 % and Carb. 0.10 %, respectively. Visualisations show in this rheo-inertial regime on one hand the presence of an asymmetric flow structure, visible on the Carb. 0.08 % visualisation insert in figure 2, and on the other hand by the pressure

ACCEPTED MANUSCRIPT
Physics of Fluids
AIP Publishing
This is the author's peer reviewed, accepted manuscript. However, the online version of record will be different from this version once it has been copyedited and typeset.
PLEASE CITE THIS ARTICLE AS DOI: 10.1063/5.0211807

signal with a change towards a dependency in $C_f \sim \mathcal{R}_w^{-0.75}$. This specific regime is called here pre-transition regime with asymmetry, as it appears before intermittency and displays an asymmetry. First puffs of the intermittent regime are seen once the critical number $\mathcal{R}_{w,c_p}$ is exceeded, here at $\mathcal{R}_{w,c_p} = 3390$ and $\mathcal{R}_{w,c_p} = 3625$ (for Carb. 0.08 and 0.10 % respectively), with a sharp break on the pressure signal ($C_f \sim \mathcal{R}_w^{-0.1}$). This intermittent regime ends at $\mathcal{R}_w = 5735$ for Carb. 0.08 % where the fully turbulent regime is reached, with strong vortices observed on visualisations and a new shift to a $C_f \sim \mathcal{R}_w^{-0.3}$ dependency. Turbulent regime data show agreement with Dodge-Metzner and Sorgun *et al.*[23] laws. However for higher concentration Carb. 0.10 %, the turbulent regime is not reached, even at maximum flowrate ($\mathcal{R}_w = 5070$), due to higher apparent viscosity.

In terms of phenomenology, visualisations on Carbopols allow to describe flow structures and therefore the rheo-inertial road to turbulence. While the laminar regime shows no differences from its Newtonian equivalent, the pre-transition regime with asymmetry, delimited by the first $\mathcal{R}_{w,c_a}$ and the second $\mathcal{R}_{w,c_p}$ critical transition Reynolds numbers, is specific to non-Newtonian fluid. Above $\mathcal{R}_{w,c_p}$, the intermittent regime begins. Figure 3(a) shows the typical transit of a turbulent puff in this regime for the Carb. 0.08 % at $\mathcal{R}_w = 3875$. At $t = t_1$ the base flow with asymmetry (line with darker light intensity below axis and lighter intensity above axis) is slowly disrupted by the arrival of the pointing edge of the puff. At $t = t_2$ the core of the puff is observed with the presence of vortices throughout this duration. At $t = t_3$, the upstream edge of the puff is seen together with flow relaminarisation back to the base flow with a re-developing asymmetry. Figure 3(b) seems to show a typical occurrence of a puff splitting event at $t = t_2$ where well-defined puff-like structures seen at $t = t_1$ and $t = t_3$ splits into two distinct puffs. In between, vortices decline after the first puff, but the flow return only partially to the base flow with residual structures close to the walls and is quickly disturbed again by the new puff pointing edge. The competition between these puff splitting events and the puff decay phenomenon is the key element to the road to turbulence, governing if the turbulence is able to be maintained as pointed out by Avila *et al.*[24].

ACCEPTED MANUSCRIPT
Physics of Fluids
AIP Publishing
This is the author's peer reviewed, accepted manuscript. However, the online version of record will be different from this version once it has been copyedited and typeset.
PLEASE CITE THIS ARTICLE AS DOI: 10.1063/5.0211807

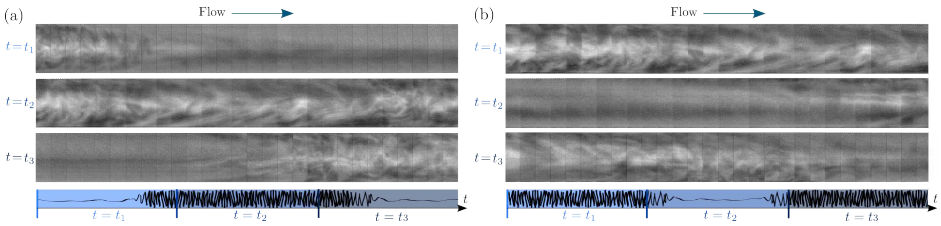

FIG. 3. Assembly of portions (width determined by the flow advection) of consecutive (4 ms interval) visualisation frames placed end to end using the Frozen Taylor hypothesis to reconstruct and enlarge the flow visualisation (width $\sim 9D$) on the Carb. 0.08 % at $\mathcal{R}_w = 3875$ for three successive times t_1, t_2 and t_3 (from top to bottom). Flow is from left to right. A schematic view over time is shown below. (a) Observation of a turbulent puff transit. (b) Observation of a puff splitting occurrence.

B. Flow asymmetry

The pre-transition regime displays a persistent asymmetry structure, as observed in the top insert in figure 2. Over the typical duration of one minute, the radial position of the line with darker light intensity than the background flow evolves slightly around a preferred position below the axis over time (as the visualisation is in the volume, the azimuthal position can not be obtained). Time-averaged grey-scale profiles $\mathcal{J}$, normalized with the centerline grey-scale level, of the central pixel column for different $\mathcal{R}_w$ from Carb. 0.10 % visualisation are shown in figure 4(a) insert, displaying a preferred overall radial position below the axis ($r/R > 0$). Main graph represents the deviation when $\mathcal{R}_w$ increase from the $\mathcal{J}_l$ laminar profile (horizontal light green line). A significant increase in deviation is observed when $\mathcal{R}_w$ increases, as well as a shift away from the axis of the preferred radial asymmetry position (curves maxima), in the pre-transitional asymmetry regime (thick blue curves). When exceeding the intermittent regime limit, profiles (dotted red curves) are tending to re-symmetrise. To approach this phenomenon, an asymmetry degree $\mathcal{A}$ is calculated from the right/left difference of the areas under the curve of the deviations and plotted with $\mathcal{R}_w$ in figure 4(b). This confirms the significant increase in the degree of flow asymmetry with $\mathcal{R}_w$ in the asymmetry regime between $\mathcal{R}_{w,c_a}$ and $\mathcal{R}_{w,c_p}$, see schematic view at the bottom. A power law fit as presented by Wen *et al.*[17] based on PIV data of the form of $a(\mathcal{R}_w - \mathcal{R}_{w,c})^b$

AIP Publishing Physics of Fluids ACCEPTED MANUSCRIPT
This is the author's peer reviewed, accepted manuscript. However, the online version of record will be different from this version once it has been copyedited and typeset.
PLEASE CITE THIS ARTICLE AS DOI: 10.1063/5.0211807

displayed as well a square-root dependence on Reynolds, with $b = 0.50$ and a R-squared value of 0.9346. Beyond $\mathcal{R}_{w,c_p}$, the asymmetry degree start decreasing as $\mathcal{R}_w$ increase, owing to the intermittent transit of turbulent puff which momentarily leads back to a symmetrical flow on average due to their vorticity.

The highlight feature of the asymmetry is that the range of $\mathcal{R}_w$ for the persistence of the asymmetry is quite large, from about 1700 to about 3625 for Carb. 0.08 % for example. Such asymmetry in pipe flow was first discussed in the context of transient growth of optimal disturbance, of the form on a blowing and suction at the wall[25]. As $\mathcal{R}_w$ increases, the disturbance grows to a larger amplitude before decaying along the pipe yet distorting the velocity field. For shear-thinning fluids, Nouar *et al.*[26] established that viscous stratification maintain laminarity and postpone the onset of transition to turbulence. Later, families of three-dimensional nonlinear traveling waves in pipe flow were obtained by Pringle and Kerswell[27]. These asymmetric modes consist in one slow streak sandwiched between two fast streaks located preferentially to one side of the pipe leading to helical and non-helical rotating waves. However, the solution with these asymmetric modes obtained numerically on a Newtonian fluid is apparently unstable enough to have never been observed experimentally in Newtonian fluids. Although, these transient and nonlinear solutions were reported for Newtonian fluids, their relevance in yield stress shear-thinning fluids is yet to be determined.

The non-linearity introduced into the behaviour law of non-Newtonian fluids may have an impact on the stability of these solutions. It could be that this state, not observed experimentally in Newtonian fluids, corresponds to the pre-transition regime with asymmetry, here stabilised by the rheology which modify their different behaviour law. It is therefore natural to wonder about the competition between the non-linearity of the rheological behaviour law and the non-linearity of the inertia term in this particular regime. The nonlinear contribution of rheological behavior shows to compete with that of the inertial term and deviating from inertial transition even for reasonably weak non-Newtonian properties, see Fig. 6. Thus, the competition seems to arise as soon as a non-negligible non-Newtonian component is introduced into the fluid.

ACCEPTED MANUSCRIPT
Physics of Fluids
AIP Publishing
This is the author's peer reviewed, accepted manuscript. However, the online version of record will be different from this version once it has been copyedited and typeset.
PLEASE CITE THIS ARTICLE AS DOI: 10.1063/5.0211807

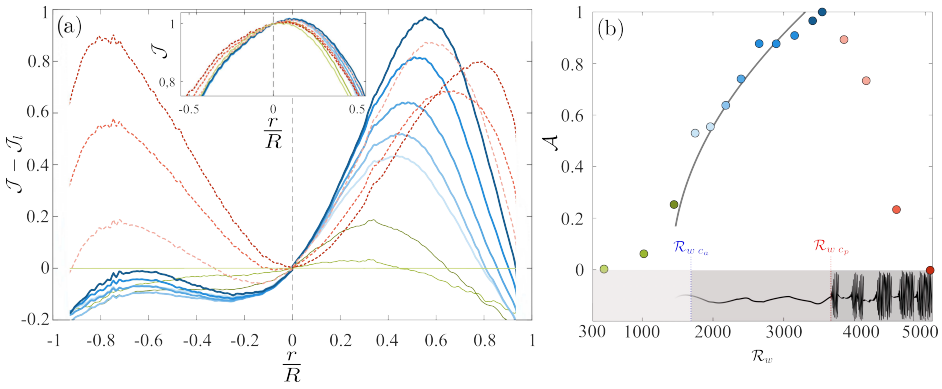

FIG. 4. (a) Grey-scale profiles $\mathcal{J}$ of the central pixel column, averaged over the recording time and normalized with the centerline level, with normalized radial position r/R for Carb. 0.10 % at different $\mathcal{R}_w$ in the top insert. Main graph represents the deviation of these profiles from the laminar profile $\mathcal{J}_l$ at minimum $\mathcal{R}_w = 415$. (b) Asymmetry degree $\mathcal{A}$ with $\mathcal{R}_w$ on the main graph. Grey curve indicate the $a(\mathcal{R}_w - \mathcal{R}_{w,c})^{0.50}$ square-root fit. A schematic view over $\mathcal{R}_w$ is shown below. In each figure, regimes are shown in color, green (thin lines) for laminar regime ($\mathcal{R}_w < \mathcal{R}_{w,c_a}$), blue (thick lines) for asymmetry regime ($\mathcal{R}_{w,c_a} < \mathcal{R}_w < \mathcal{R}_{w,c_p}$) and red (dotted lines) for turbulent regime ($\mathcal{R}_w > \mathcal{R}_{w,c_p}$).

C. Intermittency

The intermittent transit of turbulent flow structures, observed in the intermittent regime, is quantified using an intermittency indicator $I_{turb.}$. It is defined as in Rotta[28] and Avila *et al.*[24] as the fraction of time where the flow is in the turbulent state over the observation time. It provides statistical insights over an extended period concerning the proportion of turbulent flow for a given Reynolds number. It is calculated as the transit time of turbulent structures, determined by automated detection using grey-scale levels standard deviation thresholding, over the total time. $I_{turb.} = 0$ % means the absence of structure, $I_{turb.} = 100$ % means the permanent presence of structures over the duration observed, and each intermediate $I_{turb.}$ value means a percentage of intermittence. The evolution of this indicator with the flow velocity U in figure 5(a) for Carb. 0.08 %, Carb. 0.10 % and Gly./Wat. fluids shows that the intermittence differs from Newtonian to non-Newtonian, but also between non-

ACCEPTED MANUSCRIPT
Physics of Fluids
AIP Publishing
This is the author's peer reviewed, accepted manuscript. However, the online version of record will be different from this version once it has been copyedited and typeset.
PLEASE CITE THIS ARTICLE AS DOI: 10.1063/5.0211807

Newtonian fluids. To account for their respective viscosities, figure 5(b) shows the evolution with $\mathcal{R}_w$. Rotta[28] reference results for $L/D = 102$ (continuous gray curve) are shown to display the good agreement with Newtonian fluid data (green diamonds). Results follow a $\mathcal{R}_w^{\sim 0.82}$ dependency, close to the Rotta's $\mathcal{R}_w^{\sim 0.86}$ dependency. Non-Newtonian fluids show a delay in the onset to intermittence, where non-Newtonian fluids have not yet reached the intermittent regime ($I_{turb.} = 0$ %) at $\mathcal{R}_w = 3000$, whereas the fully turbulent regime has already been reached ($I_{turb.} = 100$ %) for the Newtonian fluid. The increase in the non-Newtonian behaviour between Carb. 0.08 % and 0.10 % also leads to a delay in the onset of intermittency from $\mathcal{R}_w = 3390$ to $\mathcal{R}_w = 3625$. Another phenomenon observed is the difference between the $\mathcal{R}_w^{\sim 0.82}$ dependence of the Newtonian fluid and that observed for non-Newtonian fluids, i.e. $\mathcal{R}_w^{\sim 0.73}$. Thus the transition to the turbulent regime is smoother in the presence of the non-Newtonian behaviour, which stabilises the flow. To our knowledge, this result has never been identified in the literature.

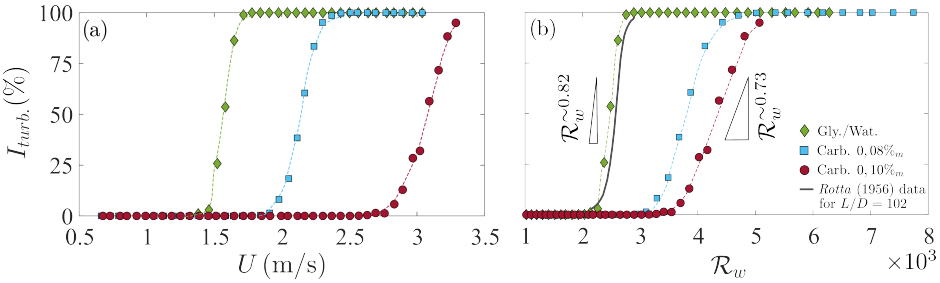

FIG. 5. Intermittency indicator $I_{turb.}$ as a function of the flow velocity U (a) and as a function of the Reynolds number $\mathcal{R}_w$ (b). Rotta[28] results for $L/D = 102$, following a $\mathcal{R}_w^{\sim 0.86}$ dependency, are shown to display the agreement with the present data. $\mathcal{R}_w$ dependencies for the Newtonian fluid (green diamonds) and for Carb. solutions (blue squares and red circles) are displayed for comparison.

D. Critical transition Reynolds numbers

One of the novelty of this work is to quantify the impact of the non-Newtonian characteristics on the delay of the rheo-inertial transition to turbulence. To summarise the previous findings, figure 6 reports $\mathcal{R}_{w,c_a}$ and $\mathcal{R}_{w,c_p}$ as a function of C, the mass concentration of

ACCEPTED MANUSCRIPT
Physics of Fluids
AIP Publishing
This is the author's peer reviewed, accepted manuscript. However, the online version of record will be different from this version once it has been copyedited and typeset.
PLEASE CITE THIS ARTICLE AS DOI: 10.1063/5.0211807

Carbopol (a), and τ_0, the yield stress (b). The schematic view at the bottom explains how the critical Reynolds numbers delimit flow regimes. The results of the present experimental investigation are compared and in good agreement with previous results of the literature for other setups and Carbopol solutions. Although a dispersion is observed, overall the results indicate that the onset of asymmetry, $\mathcal{R}_{w,c_a}$, remains almost constant with C or τ_0. However, the critical Reynolds for the appearance of puffs $\mathcal{R}_{w,c_p}$ increases linearly with C or τ_0: $\mathcal{R}_{w,c_p} = 6620 \times C + 2193$ and $\mathcal{R}_{w,c_p} = 147 \times \tau_0 + 2651$. These critical Reynolds evolutions reveal the increasing delay of the onset of turbulent puffs when the yield stress is increased. This stabilisation of the flow with a delayed transition to turbulence when the yied-stress increase is likely due to the reduction in the amplification of the kinetic energy as reported in the modal analysis of Bentrad *et al.*[29].

The onset on asymmetry seems to be related to the onset on natural disturbances. As C and τ_0 increases, the change from wall shear stress to zero shear stress on the centerline leads to large shear stress differences and stronger shear thinning that prevent disturbances to grow and propagate. Hence the disturbances modify the mean flow profile, and require higher velocities to form self-sustained puffs.

IV. CONCLUSION

In conclusion, we investigated experimentally the transition to turbulence for yield stress fluids in pipe flow and quantified rheo-inertial transition from the inertial transition of Newtonian fluids. The rheo-inertial transition displays a specific pre-transition regime with flow asymmetry, observed on both pressure drops measurements and flow visualisations between the two critical $\mathcal{R}_{w,c_a}$ and $\mathcal{R}_{w,c_p}$ Reynolds numbers. The asymmetry position drifted away from the axis as $\mathcal{R}_w$ increase and the asymmetry degree showed an increasing amplitude of asymmetry as $\mathcal{R}_w$ increase in this non-Newtonian specific regime. The intermittency indicator revealed the impacts of non-Newtonian characteristics lead to a delay on the onset of the turbulent regime towards higher $\mathcal{R}_{w,c_p}$ numbers. It revealed as well a smoother transition to turbulence, with a dependence of the intermittency on the Reynolds number that differs from the Newtonian transition one. Finally the $\mathcal{R}_{w,c_p}$ is compared to previous works, highlighting a novel observation of its linear increase with the yield stress, which delays the onset of turbulent puffs.

ACCEPTED MANUSCRIPT
Physics of Fluids
AIP Publishing
This is the author's peer reviewed, accepted manuscript. However, the online version of record will be different from this version once it has been copyedited and typeset.
PLEASE CITE THIS ARTICLE AS DOI: 10.1063/5.0211807

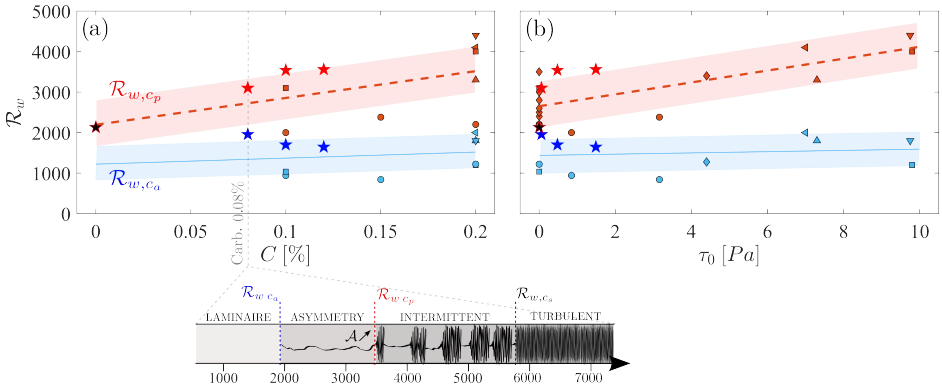

FIG. 6. Critical transition Reynolds numbers $\mathcal{R}_{w,c_a}$ and $\mathcal{R}_{w,c_p}$, as a function of the Carbopol concentration C (a) and as a function of the yield stress τ_0 for Carb. and other solutions (b), for the apparition of the asymmetry (in blue) and the apparition of puffs (in red). The data shown are taken from the present work (⋆, with Newtonian fluid in black) and from the literature: Escudier and Presti[8] (◇), Escudier *et al.*[10] (□) , Peixinho *et al.*[9] (△), Esmael and Nouar[11] (▽), Güzel *et al.*[12] (○), Bahrani and Nouar[16] (◁). Thin blue line and dotted red line show critical $\mathcal{R}_{w,c_a}$ and $\mathcal{R}_{w,c_p}$ tendencies respectively. Color bands are shown for guidance purposes. Schematic view at the bottom represents the critical Reynolds $\mathcal{R}_{w,c_a}$,$\mathcal{R}_{w,c_p}$ and $\mathcal{R}_{w,c_s}$ (onset of slugs critical Reynolds, turbulent regime) for the Carb. 0.08%.

ACKNOWLEDGMENTS

We thank C. Nouar for valuable conversations regarding the flow asymmetry discussion. Financial support of the Innovation Direction of the Greater Paris Sanitation Authority (SIAAP) in the framework of the MOCOPEE French research program (convention number: 20003867) and the Hauts-de-France French Region is gratefully acknowledged.

DATA AVAILABILITY STATEMENT

The data that support the findings of this study are available from the corresponding author upon reasonable request.

ACCEPTED MANUSCRIPT
Physics of Fluids
AIP Publishing
This is the author's peer reviewed, accepted manuscript. However, the online version of record will be different from this version once it has been copyedited and typeset.
PLEASE CITE THIS ARTICLE AS DOI: 10.1063/5.0211807

REFERENCES

[1]A. Dash and C. Poelma, "Long-time-scale transients in an industrial-scale slurry pipeline near the laminar–turbulent transition," Flow **2**, E25 (2022).

[2]Y. Dubief, V. E. Terrapon, and B. Hof, "Elasto-inertial turbulence," Annual Review of Fluid Mechanics (2022), https://doi.org/10.1146/annurev-fluid-032822-025933.

[3]W. Hogendoorn, B. Chandra, and C. Poelma, "Onset of turbulence in particle-laden pipe flows," Physical Review Fluids **7**, L042301 (2022).

[4]B. Chandra, V. Shankar, and D. Das, "Early transition, relaminarization and drag reduction in the flow of polymer solutions through microtubes," Journal of Fluid Mechanics **885**, A47 (2020).

[5]N. Agrawal, G. H. Choueiri, and B. Hof, "Transition to turbulence in particle laden flows," Physical Review Letters **122**, 114502 (2019).

[6]F. T. Pinho and J. H. Whitelaw, "Flow of non-Newtonian fluids in a pipe," Journal of Non-Newtonian Fluid Mechanics **34**, 129–144 (1990).

[7]A. Chekila, Analyse non linéaire de la stabilité de l'écoulement de Poiseuille plan d'un fluide rhéofluidifiant, Ph.D. thesis, University of Lorraine (2014).

[8]M. P. Escudier and F. Presti, "Pipe flow of a thixotropic liquid," Journal of Non-Newtonian Fluid Mechanics **62**, 291–306 (1996).

[9]J. Peixinho, C. Nouar, C. Desaubry, and B. Théron, "Laminar transitional and turbulent flow of yield stress fluid in a pipe," Journal of Non-Newtonian Fluid Mechanics **128**, 172–184 (2005).

[10]M. P. Escudier, R. J. Poole, F. Presti, C. Dales, C. Nouar, C. Desaubry, L. Graham, and L. Pullum, "Observations of asymmetrical flow behaviour in transitional pipe flow of yield-stress and other shear-thinning liquids," Journal of Non-Newtonian Fluid Mechanics **127**, 143–155 (2005).

[11]A. Esmael and C. Nouar, "Transitional flow of a yield-stress fluid in a pipe: Evidence of a robust coherent structure," Physical Review E **77**, 2–5 (2008).

[12]B. Güzel, T. Burghelea, I. A. Frigaard, and D. M. Martinez, "Observation of laminar–turbulent transition of a yield stress fluid in Hagen–Poiseuille flow," Journal of Fluid Mechanics **627**, 97–128 (2009).

ACCEPTED MANUSCRIPT
Physics of Fluids
AIP Publishing
This is the author's peer reviewed, accepted manuscript. However, the online version of record will be different from this version once it has been copyedited and typeset.
PLEASE CITE THIS ARTICLE AS DOI: 10.1063/5.0211807

[13]N. Roland, Modélisation de la transition vers la turbulence d'écoulements en tuyau de fluides rhéofluidifiants p Ph.D. thesis, University of Lorraine (2010).

[14]S. N. López-Carranza, M. Jenny, and C. Nouar, "Pipe flow of shear-thinning fluids," Comptes Rendus Mécanique **340**, 602–618 (2012).

[15]B. Hof, C. V. Doorne, J. Westerweel, F. Nieuwstadt, H. Faisst, B. Eckhardt, H. Wedin, R. Kersweli, and F. Waleffe, "Experimental observation of nonlinear traveling waves in turbulent pipe flow," Science **305**, 1594–1598 (2004).

[16]S. A. Bahrani and C. Nouar, "Intermittency in the transition to turbulence for a shear-thinning fluid in hagen-poiseuille flow," Journal of Applied Fluid Mechanics **7**, 1–6 (2014).

[17]C. Wen, R. Poole, A. P. Willis, and D. J. C. Dennis, "Experimental evidence of symmetry-breaking supercritical transition in pipe flow of shear-thinning fluids," Physical Review Fluids **2**, 1–8 (2017).

[18]C. Vavaliaris, M. Beneitez, and D. S. Henningson, "Optimal perturbations and transition energy thresholds in boundary layer shear flows," Physical Review Fluids **5**, 062401 (2020).

[19]M. Beneitez, Y. Duguet, P. Schlatter, and D. S. Henningson, "Instability of the optimal edge trajectory in the blasius boundary layer," Journal of Fluid Mechanics **971** (2023), https://doi.org/10.1017/jfm.2023.545.

[20]G. B. Froishteter and G. V. Vinogradov, "The laminar flow of plastic disperse systems in circular tubes," Rheologica Acta **19**, 239–250 (1980).

[21]J. M. Piau, "Carbopol gels: Elastoviscoplastic and slippery glasses made of individual swollen sponges. meso- and macroscopic properties, constitutive equations and scaling laws," Journal of Non-Newtonian Fluid Mechanics **144**, 1–29 (2007).

[22]N. Abcha, N. Latrache, F. Dumouchel, and I. Mutabazi, "Qualitative relation between reflected light intensity by kalliroscope flakes and velocity field in the couette-taylor flow system," Experiments in Fluids **45**, 85–94 (2008).

[23]M. Sorgun, T. D. Muftuoglu, and I. H. Gucuyener, "Friction factor estimation for turbulent flow of Herschel-Bulkley and power law fluids in pipes," Journal of Petroleum Science and Engineering **211**, 110044 (2022).

[24]M. Avila, D. Barkley, and B. Hof, "Transition to turbulence in pipe flow," Annual Review of Fluid Mechanics **5**, 575–602 (2022).

[25]M. I. Gavarini, A. Bottaro, and F. T. M. Nieuwstadt, "Optimal and robust control of streaks in pipe flow," Journal of Fluid Mechanics **537**, 187–219 (2005).

AIP Publishing Physics of Fluids ACCEPTED MANUSCRIPT
This is the author's peer reviewed, accepted manuscript. However, the online version of record will be different from this version once it has been copyedited and typeset.
PLEASE CITE THIS ARTICLE AS DOI: 10.1063/5.0211807

[26]C. Nouar, A. Bottaro, and J. P. Brancher, "Delaying transition to turbulence in channel flow: Revisiting the stability of shear thinning fluids," Journal of Fluid Mechanics **592**, 177–194 (2007).

[27]C. C. T. Pringle and R. R. Kerswell, "Asymmetric, helical, and mirror-symmetric traveling waves in pipe flow," Physical Review Letters **99**, 074502 (2007).

[28]J. Rotta, "Experimenteller beitrag zur entstehung turbulenter strömung im rohr," Ingenieur-Archiv **24**, 258–281 (1956).

[29]H. Bentrad, A. Esmael, C. Nouar, A. Lefevre, and N. Ait-Messaoudene, "Energy growth in hagen-poiseuille flow of herschel-bulkley fluid," Journal of Non-Newtonian Fluid Mechanics **241**, 43–59 (2017).